Time-domain approach to the forward scattering sum rule

Gustafsson, Mats

2010

CODEN:LUTEDX/(TEAT-7185)/1-14/(2010)

Revision No. 1: April 2010

Time-domain approach to the forward scattering sum rule

Mats Gustafsson

Electromagnetic Theory
Department of Electrical and Information Technology
Lund University
Sweden

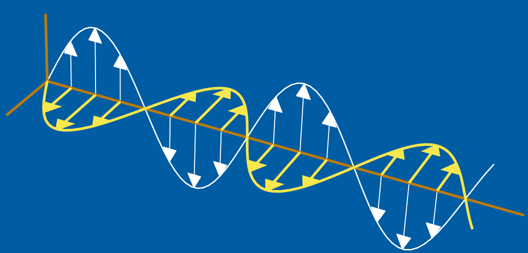

Mats Gustafsson
Mats.Gustafsson@eit.lth.se

Department of Electrical and Information Technology
Electromagnetic Theory
Lund University
P.O. Box 118
SE-221 00 Lund
Sweden

Editor: Gerhard Kristensson

Abstract

The forward scattering sum rule relates the extinction cross section integrated over all wavelengths with the polarizability dyadics. It is useful for deriving bounds on the interaction between scatterers and electromagnetic fields, antenna bandwidth and directivity, and energy transmission through sub-wavelength apertures. The sum rule is valid for linearly polarized plane waves impinging on linear, passive, and time translational invariant scattering objects in free space. Here, a time-domain approach is used to clarify the derivation and the used assumptions. The time-domain forward scattered field defines an impulse response. Energy conservation shows that this impulse response is the kernel of a passive convolution operator that implies that the Fourier transform of the impulse response is a Herglotz function. The forward scattering sum rule is finally constructed from integral identities for Herglotz functions.

1 Introduction

The forward scattering sum rule relates the extinction cross section integrated over all wavelengths with the polarizability of the scatterer defined by its electric and magnetic polarizability dyadics. This sum rule was introduced for spheroidal dielectrics in [22] and generalized to arbitrary heterogeneous objects in [26]. Related dispersion relations are considered by several authors, see *e.g.*, [19–21]. In addition to the insight the identity provides in scattering theory, it offers physical bounds on the interaction between arbitrary obstacles and electromagnetic fields [26]. For example, it is useful in the analysis of metamaterials where it shows that an increased interaction is traded against bandwidth [27, 28]. It has also been used to demonstrate how size and shape affect performance in antenna theory [4, 9, 10, 25] and for extra-ordinary transmission of energy though sub wavelength apertures [12].

Here, a time-domain derivation of the forward scattering sum rule is presented. The derivation is based on transient scattering of an incident plane wave in the form of a (Dirac) delta pulse. The scattered field of an ordinary incident pulse with finite power density is retrieved from convolution between the impulse response and the pulse shape. Moreover, the corresponding time-harmonic forward scattered field is obtained from a multiplication with the transfer function, *i.e.*, the Fourier transform of the impulse response. These properties are related to the impulse response and transfer function that are commonly used in linear system theory [31]. The sum rule relates the extincted (*i.e.*, the scattered and absorbed) power of an object integrated over all wavelengths with the polarizability of the object times the incident power flux. The corresponding physical bounds show that the bandwidth times the extinction is bounded by the polarizability. Moreover, the polarizability dyadic of an object is bounded by the high-contrast polarizability dyadic that only depends on the geometry of the object [26]. This demonstrates that large extinction cross sections of sub-wavelength objects are only possible over limited frequency intervals.

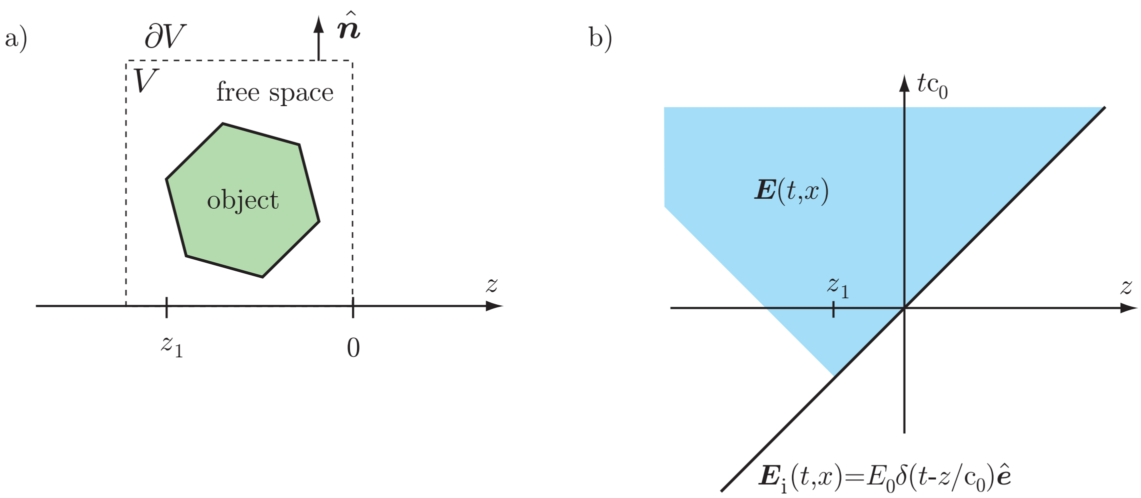

Figure 1: a) a scattering object confined to the region $[z_1, 0]$ together with a circumscribing surface, ∂V, with unit normal vector $\hat{\boldsymbol{n}}$. b) region that contains the spatial and temporal support of the field.

The time-domain analysis shows that, under the assumption of passivity, the impulse response is the kernel of a passive convolution operator [31]. The corresponding transfer function is then a positive real function [8, 31] or a Herglotz [20] (or Nevanlinna or Pick [5]) function. This choice depends on the considered right or upper complex half plane that is often induced by the time conventions $e^{j\omega t}$ and $e^{-i\omega t}$, respectively, where $i^2 = -1$ and $j = -i$. Here, Herglotz functions are considered [20]. They are defined as holomorphic mappings from the upper complex half plane into itself. Integral identities for Herglotz functions are used to derive the forward scattering sum rule [2, 7, 9, 26]. It is straight forward to transform the derivation to positive real functions [31] using the time convention $e^{j\omega t}$.

This paper is organized as follows. In Sec. 2, the forward scattering impulse response is introduced and the extincted energy of an incident time-domain plane wave is derived. The corresponding results in the frequency domain are analyzed in Sec. 3. Sum rules, related physical bounds, and numerical examples are given in Sec. 4. Sec. 5 contains the conclusions.

2 Time domain forward scattering

Introduce a coordinate system such that the finite scattering object is confined to the region $z_1 \leq z \leq 0$ leaving $z \geq 0$ as free space, see Fig 1a. Consider a transient incident plane wave in the form of a (Dirac) delta distribution, δ, propagating in the z-direction, *i.e.*, the incident electric and magnetic field intensities are

$$\boldsymbol{E}_i^{(\delta)}(t, \boldsymbol{r}) = \hat{\boldsymbol{e}}\delta(t - z/c_0) \quad \text{and} \quad \boldsymbol{H}_i^{(\delta)}(t, \boldsymbol{r}) = \eta_0^{-1}\hat{\boldsymbol{z}} \times \hat{\boldsymbol{e}}\delta(t - z/c_0), \tag{2.1}$$

respectively, where $\hat{\boldsymbol{e}} \cdot \hat{\boldsymbol{z}} = 0$, c_0 denotes the speed of light in free space, and η_0 is the intrinsic impedance of free space. The spatial and temporal support (the support

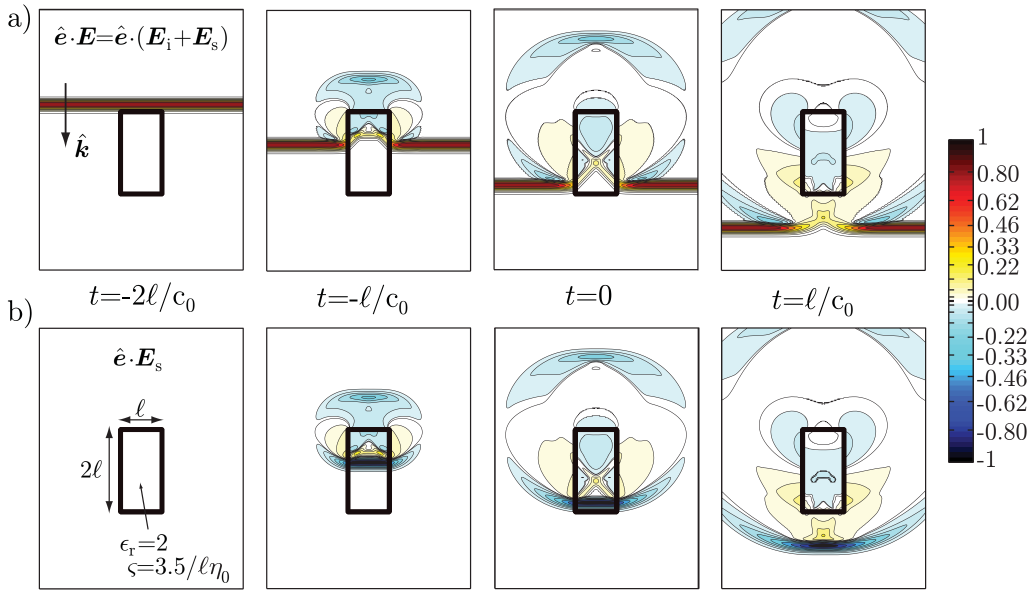

Figure 2: Snapshots illustrating the scattering of an incident Gaussian pulse by a dielectric brick with relative permittivity $\epsilon_r = 2$ and conductivity $\varsigma = 3.5/\ell\eta_0$ using FDTD. a) total field $\hat{\boldsymbol{e}} \cdot \boldsymbol{E}(t, \boldsymbol{r})$. b) scattered field $\hat{\boldsymbol{e}} \cdot \boldsymbol{E}_s(t, \boldsymbol{r})$.

is the region where the field is non-zero) of the incident field is given by the plane defined by $t = z/c_0$, see Fig 1b. The (total) field is equal to the incident field until the pulse reaches the object, *i.e.*, for $t < z_1/c_0$. The support of the field is more complex for larger times due to the interaction between the incident field and the object. In general, it requires a solution of the Maxwell equations with an accurate model of the constitutive relations to determine the field and its support, see *e.g.*, Fig. 2a and Fig. 3. However, for the purpose of deriving the forward scattering sum rule, it is sufficient to determine a region that contains the support of the field, see Fig 1b. This region is solely based on the fundamental property that the wavefront velocity is bounded by the speed of light in free space and that the incident wave does not reach the object until the time $t = z_1/c_0$.

Before specific material models of the scattering object and the Maxwell equations are considered it is important to review the underlying physics that the constitutive relations should fulfill. A fundamental property is that the propagation of an electromagnetic wave is limited by the speed of light in free space. Note that this is a bound on the wavefront velocity and not the phase velocity or group velocity that are commonly used for time harmonic fields. The wavefront velocity quantifies the speed that the wavefront propagates with in the direction orthogonal to itself. This is related to the Huygens principle that states that each point of an advancing wavefront is the center of a new disturbance [6].

Mathematically, it is necessary to consider a set of constitutive relations that guarantee these properties when used together with the Maxwell equations. Here, the analysis is restricted to linear, time translational invariant, continuous, passive, isotropic, and non-magnetic material models for simplicity. This gives the temporally dispersive constitutive relations of the form

$$\boldsymbol{D}(t,\boldsymbol{r}) = \epsilon_0\epsilon_\infty(\boldsymbol{r})\boldsymbol{E}(t,\boldsymbol{r}) + \epsilon_0\int_0^\infty \chi_{\mathrm{t}}(t',\boldsymbol{r})\boldsymbol{E}(t-t',\boldsymbol{r})\,\mathrm{d}t' \tag{2.2}$$

and $\boldsymbol{B} = \mu_0\boldsymbol{H}$, where ϵ_0 and μ_0 denote the intrinsic permittivity and permeability of free space, respectively, $\epsilon_\infty(\boldsymbol{r}) \geq 1$ is the instantaneous response, and χ_{t} the electric susceptibility kernel. To guarantee a well posed solution of the Maxwell equations, it is also assumed that $|\frac{\partial\chi_{\mathrm{t}}}{\partial t}|$ is integrable in t. The instantaneous response models the direct response of the medium whereas the susceptibility kernel models the temporal dispersion. One can argue that $\epsilon_\infty = 1$ for materials as the medium cannot react instantaneously to the electromagnetic field [13]. However, here the general case with an arbitrary $\epsilon_\infty \geq 1$ is considered. This is motivated from a modeling point of view where ϵ_∞ is the permittivity for sufficiently high frequencies (or equivalently fast temporal responses) compared with the frequency range of interest [11].

The wave-front velocity in the medium is now given by $\mathrm{c}_0/\sqrt{\epsilon_\infty(\boldsymbol{r})} \leq \mathrm{c}_0$. This is easily understood for the plane-wave solution in a homogeneous medium. General inhomogeneous objects require further analysis, where the general properties follow from the analysis of symmetric hyperbolic systems [6, 18] together with the observation that the principal part of the Maxwell equations determine the propagation of the wavefront. This reduces the analysis to the case of non-dispersive material models, *i.e.*, $\chi_{\mathrm{t}} = 0$ in (2.2).

Decompose the (total) field into incident and scattered fields as

$$\boldsymbol{E}^{(\delta)}(t,\boldsymbol{r}) = \boldsymbol{E}_{\mathrm{i}}^{(\delta)}(t,\boldsymbol{r}) + \boldsymbol{E}_{\mathrm{s}}^{(\delta)}(t,\boldsymbol{r}) \quad \text{and } \boldsymbol{H}^{(\delta)}(t,\boldsymbol{r}) = \boldsymbol{H}_{\mathrm{i}}^{(\delta)}(t,\boldsymbol{r}) + \boldsymbol{H}_{\mathrm{s}}^{(\delta)}(t,\boldsymbol{r}), \tag{2.3}$$

see also the numerical example in Fig. 2. The surface integral representation (.6) of the scattered field is used to determine the co-polarized scattered far-field in the forward direction as $\hat{\boldsymbol{e}}\cdot\boldsymbol{F}^{(\delta)}(t,\hat{\boldsymbol{z}}) = -\frac{\partial h_{\mathrm{t}}}{\partial t}/4\pi\mathrm{c}_0$, where

$$h_{\mathrm{t}}(t) = \hat{\boldsymbol{e}}\cdot\int_{\partial V} \hat{\boldsymbol{z}}\times\big(\hat{\boldsymbol{n}}(\boldsymbol{r})\times\boldsymbol{E}_{\mathrm{s}}^{(\delta)}(t+z/\mathrm{c}_0,\boldsymbol{r})\big) + \eta_0\hat{\boldsymbol{n}}(\boldsymbol{r})\times\boldsymbol{H}_{\mathrm{s}}^{(\delta)}(t+z/\mathrm{c}_0,\boldsymbol{r})\,\mathrm{dS}\,. \tag{2.4}$$

It is realized that the field of an incident δ-pulse does not decay according to the inverse square law. However, the far-field of an incident square integrable pulse is determined by convolution of the pulse shape with the impulse response as outlined in 5.

The surface representation (2.4) is used to show that h_{t} is causal, *i.e.*, $h_{\mathrm{t}}(t) = 0$ for $t < 0$. Here, it is convenient to consider the scattered field on the surface defined by $z = 0$ with $\hat{\boldsymbol{n}} = \hat{\boldsymbol{z}}$, that simplifies the surface integral representation (2.4) into

$$h_{\mathrm{t}}(t) = -\int_{\mathbb{R}^2} \hat{\boldsymbol{e}}\cdot\boldsymbol{E}_{\mathrm{s}}^{(\delta)}(t,\boldsymbol{r}) + \eta_0(\hat{\boldsymbol{z}}\times\hat{\boldsymbol{e}})\cdot\boldsymbol{H}_{\mathrm{s}}^{(\delta)}(t,\boldsymbol{r})\,\mathrm{dS}, \tag{2.5}$$

where $\boldsymbol{r}\cdot\hat{\boldsymbol{z}} = 0$. It is seen that h_{t} is the component of the scattered field that is co-polarized with the incident field at $z = 0$. The properties of $h_{\mathrm{t}}(t)$ can hence be

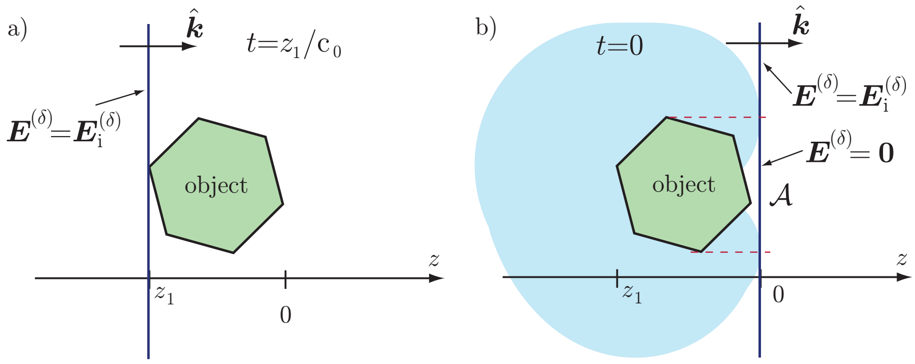

Figure 3: Snapshots of the spatial support of the field $\boldsymbol{E}^{(\delta)}(t,\boldsymbol{r})$. a) at $t=z_1/c_0$, *i.e.*, the pulse reaches the object. b) at $t=0$, *i.e.*, the pulse has passed the object.

obtained from the corresponding properties of the scattered field. It is obvious that $h_{\rm t}(t)$ is quiescent for $t<0$ as the same holds for the scattered field as well as for the total field.

The impulse response in the forward direction $h_{\rm t}(t)$ is now used to express the extincted energy, *cf.*, the time-domain optical theorem [3, 15]. A compactly supported smooth pulse shape, $E(t)$, is considered to ensure that the extincted energy is well defined. The total and scattered fields induced by the incident field,

$$\boldsymbol{E}_{\rm i}(t,\boldsymbol{r})=\hat{\boldsymbol{e}}E(t-z/c_0) \tag{2.6}$$

is represented as a convolution between the impulse response, $\boldsymbol{E}_{\rm s}^{(\delta)}$, and the incident pulse shape, *i.e.*,

$$\boldsymbol{E}_{\rm s}(t,\boldsymbol{r})=\int_{\mathbb{R}}\boldsymbol{E}_{\rm s}^{(\delta)}(t-\tau,\boldsymbol{r})E(\tau)\,{\rm d}\tau \tag{2.7}$$

and similarly for $\boldsymbol{H}_{\rm s}$. The extincted energy, $W_{\rm ext}$, is the sum of the absorbed and scattered energies. The scattered energy at time T with respect to the region V is defined as the energy of the scattered field outside V, *i.e.*,

$$\frac{1}{2}\int_{\mathbb{R}^3\setminus V}\epsilon_0|\boldsymbol{E}_{\rm s}(T,\boldsymbol{r})|^2+\mu_0|\boldsymbol{H}_{\rm s}(T,\boldsymbol{r})|^2\,{\rm dV} \\ =\int_{-\infty}^{T}\int_{\partial V}\big(\boldsymbol{E}_{\rm s}(t,\boldsymbol{r})\times\boldsymbol{H}_{\rm s}(t,\boldsymbol{r})\big)\cdot\hat{\boldsymbol{n}}(\boldsymbol{r})\,{\rm dS}\,{\rm d}t, \tag{2.8}$$

where the equality follows from conservation of energy in the form of the Poynting's theorem [13, 30]. Similarly, the absorbed energy is defined as the difference between the total energy and the incident energy in V

$$\int_{-\infty}^{T}\int_{V}\boldsymbol{E}\cdot\frac{\partial\boldsymbol{D}}{\partial t}+\boldsymbol{H}\cdot\frac{\partial\boldsymbol{B}}{\partial t}-\epsilon_0\boldsymbol{E}_{\rm i}\cdot\frac{\partial\boldsymbol{E}_{\rm i}}{\partial t}-\mu_0\boldsymbol{H}_{\rm i}\cdot\frac{\partial\boldsymbol{H}_{\rm i}}{\partial t}\,{\rm dV}\,{\rm d}t \\ =-\int_{-\infty}^{T}\int_{\partial V}\big(\boldsymbol{E}(t,\boldsymbol{r})\times\boldsymbol{H}(t,\boldsymbol{r})-\boldsymbol{E}_{\rm i}(t,\boldsymbol{r})\times\boldsymbol{H}_{\rm i}(t,\boldsymbol{r})\big)\cdot\hat{\boldsymbol{n}}(\boldsymbol{r})\,{\rm dS}\,{\rm d}t. \tag{2.9}$$

Note that the absorbed and scattered energies at a time T depend on the considered region V. Now the extincted energy can be written as an integral of the energy flux through the surface ∂V, *i.e.*,

$$\begin{aligned}
&W_{\text{ext}}(T)\\
&= -\int_{-\infty}^{T}\int_{\partial V} \big(\boldsymbol{E}(t,\boldsymbol{r})\times\boldsymbol{H}(t,\boldsymbol{r})-\boldsymbol{E}_{\text{s}}(t,\boldsymbol{r})\times\boldsymbol{H}_{\text{s}}(t,\boldsymbol{r})-\boldsymbol{E}_{\text{i}}(t,\boldsymbol{r})\times\boldsymbol{H}_{\text{i}}(t,\boldsymbol{r})\big)\cdot\hat{\boldsymbol{n}}(\boldsymbol{r})\,\mathrm{dS}\,\mathrm{d}t\\
&\quad= -\int_{-\infty}^{T}\int_{\partial V} \big(\boldsymbol{E}_{\text{i}}(t,\boldsymbol{r})\times\boldsymbol{H}_{\text{s}}(t,\boldsymbol{r})+\boldsymbol{E}_{\text{s}}(t,\boldsymbol{r})\times\boldsymbol{H}_{\text{i}}(t,\boldsymbol{r})\big)\cdot\hat{\boldsymbol{n}}(\boldsymbol{r})\,\mathrm{dS}\,\mathrm{d}t. \qquad (2.10)
\end{aligned}$$

This form is used in the time-domain version of the optical theorem [15]. It is observed that $W_{\text{ext}}(T)$ is independent of T for large times as $\boldsymbol{E}_{\text{i}}$ and $\boldsymbol{H}_{\text{i}}$ in (2.10) are quiescent after the incident pulse has passed the region V. In particular, this implies that $W_{\text{ext}}(\infty)\geq 0$ is independent of the considered region V. The sign $W_{\text{ext}}(\infty)\geq 0$ follows directly from the non-negative signs of (2.8) and (2.9), where the passivity of the constitutive relations (2.2) and the finite support of $E(t)$ are used.

Use (2.6) and the relation (2.7) of the scattered field to rewrite the extincted energy as

$$\begin{aligned}
W_{\text{ext}}(T) &= -\int_{-\infty}^{T}\int_{\partial V} \hat{\boldsymbol{z}}\cdot\big(\hat{\boldsymbol{e}}\times\boldsymbol{H}_{\text{s}}(\tau,\boldsymbol{r})\big)+\big(\boldsymbol{E}_{\text{s}}(\tau,\boldsymbol{r})\times(\hat{\boldsymbol{z}}\times\hat{\boldsymbol{e}})\big)\cdot\hat{\boldsymbol{z}}/\eta_0\,\mathrm{dS}\,E(\tau)\,\mathrm{d}\tau\\
&= -\int_{-\infty}^{T}\int_{\mathbb{R}}\int_{\partial V} (\hat{\boldsymbol{z}}\times\hat{\boldsymbol{e}})\cdot\boldsymbol{H}_{\text{s}}^{(\delta)}(\tau-t,\boldsymbol{r})+\hat{\boldsymbol{e}}\cdot\boldsymbol{E}_{\text{s}}^{(\delta)}(\tau-t,\boldsymbol{r})/\eta_0\,\mathrm{dS}\,E(\tau)E(t)\,\mathrm{d}t\,\mathrm{d}\tau\\
&= \frac{1}{\eta_0}\int_{-\infty}^{T}\int_{\mathbb{R}} E(t)h_{\text{t}}(\tau-t)E(\tau)\,\mathrm{d}t\,\mathrm{d}\tau, \qquad (2.11)
\end{aligned}$$

where the surface is chosen as the surface $z=0$ and h_{t} is identified from the surface integral representation of the scattered field in the forward direction (2.5). This relation is valid for all compactly supported smooth functions $E(t)$, and $W_{\text{ext}}(\infty)\geq 0$ classifies the impulse response, $h_{\text{t}}(t)$, as a (tempered) distribution of positive type [23]. Passivity and the finite speed of propagation is now used to show that $W_{\text{ext}}(T)\geq 0$ for all $E(t)$. The extincted energy (2.10) is first rewritten as a volume integral over the exterior region, *i.e.*,

$$\begin{aligned}
W_{\text{ext}}(T) = \frac{1}{2}\int_{\mathbb{R}^3\setminus V} &\epsilon_0\big(|\boldsymbol{E}_{\text{i}}(T,\boldsymbol{r})|^2+|\boldsymbol{E}_{\text{s}}(T,\boldsymbol{r})|^2-|\boldsymbol{E}(T,\boldsymbol{r})|^2\big)\\
&+\mu_0\big(|\boldsymbol{H}_{\text{i}}(T,\boldsymbol{r})|^2+|\boldsymbol{H}_{\text{s}}(T,\boldsymbol{r})|^2-|\boldsymbol{H}(T,\boldsymbol{r})|^2\big)\,\mathrm{dV}. \qquad (2.12)
\end{aligned}$$

Using (2.12) with $\mathbb{R}^3\setminus V$ as the region $z\geq 0$, it follows that $W_{\text{ext}}(T)\geq 0$. This characterizes $h_{\text{t}}(t)$ as the kernel of a passive convolution operator [31], that has the general representation [31]

$$h_{\text{t}}(t) = B\delta'(t)+\theta(t)\int_{\mathbb{R}}\cos(\xi t)\,\mathrm{d}\beta(\xi), \qquad (2.13)$$

where $B \geq 0$, $\theta(t) = 0$ for $t < 0$, $\theta(t) = 1$ for $t > 0$, and $\mathrm{d}\beta(\xi)/(1+\xi^2)$ is a finite measure, *i.e.*, $\int_{\mathbb{R}} (1+\xi^2)^{-1} \,\mathrm{d}\beta(\xi) < \infty$.

The constant B in (2.13) is further restricted. The finite speed of propagation restricts the surface integral (2.5) to the projection of the geometrical cross section on the surface $z = 0$ for short times, *i.e.*, as $t \to 0$. It also creates a shadow zone, denoted by $\mathcal{A}$ in Fig. 3b, where $\boldsymbol{E}^{(\delta)}(t, \boldsymbol{r}) = \eta_0 \boldsymbol{H}^{(\delta)}(t, \boldsymbol{r}) = \mathbf{0}$, behind impenetrable objects or objects with $\epsilon_\infty > 1$, causing $\boldsymbol{E}_{\mathrm{s}}^{(\delta)}(t, \boldsymbol{r}) = -\boldsymbol{E}_{\mathrm{i}}^{(\delta)}(t, \boldsymbol{r}) = -\hat{\boldsymbol{e}}\delta(t)$ and $\boldsymbol{H}_{\mathrm{s}}^{(\delta)}(t, \boldsymbol{r}) = -\boldsymbol{H}_{\mathrm{i}}^{(\delta)}(t, \boldsymbol{r}) = -\eta_0^{-1} \hat{\boldsymbol{z}} \times \hat{\boldsymbol{e}}\delta(t)$ as $t \to 0$ in this region. This gives a short time behavior of the form $h_{\mathrm{t}}(t) \approx 2A\delta(t)$ as $t \to 0$ for these types of objects, where $A = \int_{\mathcal{A}} \mathrm{dS}$ denotes the area of $\mathcal{A}$, *cf.*, the extinction paradox. This shows that $B = 0$ in (2.13).

3 Fourier domain forward scattering

The derivation of the forward scattering sum rule is based on integral identities in the Fourier domain [26]. A Fourier transform of the impulse response, h_{t}, defines $h(k)$ as

$$h(k) = \mathrm{i} \int_{\mathbb{R}} h_{\mathrm{t}}(t) \mathrm{e}^{\mathrm{i}ktc_0} \,\mathrm{d}t, \tag{3.1}$$

where $k = \omega/\mathrm{c}_0$ with $\operatorname{Im} k > 0$ denotes the wavenumber and the multiplication with the imaginary unit, i, is used to rotate the range to the upper complex half plane. The Fourier (Laplace) transform of $h_{\mathrm{t}}(t)$ defined by (2.13) classifies $h(k)$ as a (symmetric) Herglotz function [2, 5, 20], that can be represented by the integral

$$h(k) = Bk + \int_{\mathbb{R}} \frac{1}{\xi - k} - \frac{\xi}{1+\xi^2} \,\mathrm{d}\beta(\xi) = Bk + \int_{\mathbb{R}} \frac{k}{\xi^2 - k^2} \,\mathrm{d}\beta(\xi), \tag{3.2}$$

where $\operatorname{Im} k > 0$ and $\int_{\mathbb{R}} (1+\xi^2)^{-1} \,\mathrm{d}\beta(\xi) < \infty$ [20, 31]. The cross symmetry $h(k) = -h^*(-k^*)$ used in (3.2), where a star denotes the complex conjugate, follows from the real valued h_{t}. It is observed that $\mathrm{d}\beta(\xi) = \operatorname{Im} h(\xi) \,\mathrm{d}\xi/\pi$ if $\operatorname{Im} h(\xi)$ is sufficiently regular [5] offering a simple relation with the Hilbert transform and the Kramers-Kronig relations [13, 16]. A Herglotz function is holomorphic in $\operatorname{Im} k > 0$ and its imaginary part is non-negative, $\operatorname{Im} h(k) \geq 0$, *i.e.*, $h(k)$ maps the upper half plane into itself. The high frequency limit is $h(k)/k \to B \geq 0$ as $k \hat{\to} \infty$, where $\hat{\to}$ is a shorthand notation for limits such that $\alpha \leq \arg(k) < \pi - \alpha$ for some $\alpha > 0$.

The Plancherel formula expresses the extincted energy (2.11) as

$$W_{\mathrm{ext}}(\infty) = \frac{\mathrm{c}_0}{2\pi\eta_0} \int_{\mathbb{R}} \operatorname{Im} h(k) |\widetilde{\boldsymbol{E}}_{\mathrm{i}}(k)|^2 \,\mathrm{d}k = \frac{\mathrm{c}_0}{2\pi\eta_0} \int_{\mathbb{R}} \sigma_{\mathrm{ext}}(k; \hat{\boldsymbol{k}}, \hat{\boldsymbol{e}}) |\widetilde{\boldsymbol{E}}_{\mathrm{i}}(k)|^2 \,\mathrm{d}k, \tag{3.3}$$

where $\sigma_{\mathrm{ext}}(k) = \operatorname{Im} h(k)$ is the extinction cross section. The extinction cross section of an object is also related to the forward scattering of the object via the optical theorem [19, 20], *i.e.*, $\sigma_{\mathrm{ext}}(k) = \operatorname{Im} h(k)$, where $h(k) = 4\pi \hat{\boldsymbol{e}} \cdot \widetilde{\boldsymbol{F}}^{(\delta)}(k; \hat{\boldsymbol{k}})/k$ and $\widetilde{\boldsymbol{F}}^{(\delta)}$ denotes the far-field amplitude. The function $h(k)$ can hence be considered as a holomorphic continuation of $\sigma_{\mathrm{ext}}(k)$ into $\operatorname{Im} k > 0$.

The surface integral representation of the electromagnetic field expresses the far field in the scattered field on the surface $z = 0$, *cf.*, (2.5). Written in the function $h(k)$ it reads

$$h(k) = -\mathrm{i} \int_{\mathbb{R}^2} \hat{\boldsymbol{e}} \cdot \widetilde{\boldsymbol{E}}_{\mathrm{s}}^{(\delta)}(k, \boldsymbol{r}) + \eta_0 (\hat{\boldsymbol{z}} \times \hat{\boldsymbol{e}}) \cdot \widetilde{\boldsymbol{H}}_{\mathrm{s}}^{(\delta)}(k, \boldsymbol{r}) \,\mathrm{dS}, \tag{3.4}$$

where the incident wave is the unit-amplitude time-harmonic plane wave $\widetilde{\boldsymbol{E}}_{\mathrm{i}}^{(\delta)}(k, \boldsymbol{r}) = \mathrm{e}^{\mathrm{i}kz}\hat{\boldsymbol{e}}$ and $\widetilde{\boldsymbol{E}}_{\mathrm{s}}^{(\delta)}$ and $\widetilde{\boldsymbol{H}}_{\mathrm{s}}^{(\delta)}$ denote the Fourier transforms of $\boldsymbol{E}_{\mathrm{s}}^{(\delta)}$ and $\boldsymbol{H}_{\mathrm{s}}^{(\delta)}$, respectively.

The low-frequency asymptotic expansion of the far field is well known and *e.g.*, analyzed in [17]. Here, a simplified derivation based on the volume integral representation (.2) is presented, see [17] for a more general derivation. It is valid for the constitutive relations (2.2) without a static conductivity. The low-frequency asymptotic expansions $\mathrm{e}^{-\mathrm{i}k\hat{\boldsymbol{k}}\cdot\boldsymbol{r}} = 1 + \mathcal{O}(k)$ and $\widetilde{\boldsymbol{E}}^{(\delta)} = \widetilde{\boldsymbol{E}}_0^{(\delta)} + \mathcal{O}(k)$ as $k \to 0$ together with the induced current $\eta_0 \widetilde{\boldsymbol{J}}^{(\delta)}(k, \boldsymbol{r}) = -\mathrm{i}k(\epsilon_{\mathrm{r}}(k, \boldsymbol{r}) - 1)\widetilde{\boldsymbol{E}}^{(\delta)}(k, \boldsymbol{r})$ inserted into the volume integral representation (.2) are used to get

$$h(k) = \mathrm{i}\eta_0 \int_V \hat{\boldsymbol{e}} \cdot \widetilde{\boldsymbol{J}}^{(\delta)}(k, \boldsymbol{r}) \mathrm{e}^{-\mathrm{i}k\hat{\boldsymbol{k}}\cdot\boldsymbol{r}} \,\mathrm{dV} = k\hat{\boldsymbol{e}} \cdot \int_V (\epsilon_{\mathrm{r}}(0, \boldsymbol{r}) - 1) \widetilde{\boldsymbol{E}}_0^{(\delta)}(\boldsymbol{r}) \,\mathrm{dV} + \mathcal{O}(k^2)$$
$$= k\hat{\boldsymbol{e}} \cdot \boldsymbol{\gamma}_{\mathrm{e}} \cdot \hat{\boldsymbol{e}} + \mathcal{O}(k^2) \quad \text{as } k \to 0, \tag{3.5}$$

where $\boldsymbol{\gamma}_{\mathrm{e}}$ denotes the electric polarizability dyadic [17, 30].

The high frequency asymptotic is more involved. Obviously, the high-frequency response depends on the corresponding high-frequency limit of the constitutive relations. As discussed above it is sometimes argued that the constitutive relations reduce to their free space values in this limit. This would simplify the analysis, however, here the general constitutive relations (2.2) are considered. The representation (3.2) shows that it is sufficient to consider the high frequency asymptote on the imaginary axis $k' = 0$ as $k'' \to \infty$, where $k = k' + \mathrm{i}k''$. The high-frequency asymptotic is hence related to the short time behavior of $h_{\mathrm{t}}(t)$ since

$$h(\mathrm{i}k'') = \mathrm{i} \int_0^{\tau_1} \mathrm{e}^{-k'' t c_0} h_{\mathrm{t}}(t) \,\mathrm{d}t + \mathrm{i}\mathrm{e}^{-k''\tau_1 c_0} \int_0^{\infty} \mathrm{e}^{-k'' t c_0} h_{\mathrm{t}}(t + \tau_1) \,\mathrm{d}t \tag{3.6}$$

for any $\tau_1 > 0$. The second integral decays exponentially with k'', so the high frequency asymptotic is given by the first integral with an arbitrary small τ_1. The short time response of (2.5) shows that $h_{\mathrm{t}}(t) \approx 2A\delta(t)$ as $t \to 0$ for impenetrable objects and hence $h(k) \to 2A\mathrm{i}$ as $k'' \to \infty$, where A denotes the cross section area of the shadow zone $\mathcal{A}$, see Fig. 3.

4 Sum rules and physical bounds

Integrate $h(k)$ over a line in the upper complex half plane and use the low-frequency asymptote (3.5) to get the sum rule [2, 26]

$$\lim_{\varepsilon \to 0} \lim_{y \to 0} \frac{2}{\pi} \int_{\varepsilon}^{\infty} \frac{\sigma_{\mathrm{ext}}(k + \mathrm{i}y; \hat{\boldsymbol{k}}, \hat{\boldsymbol{e}})}{k^2} \,\mathrm{d}k = \frac{2}{\pi} \int_0^{\infty} \frac{\sigma_{\mathrm{ext}}(k; \hat{\boldsymbol{k}}, \hat{\boldsymbol{e}})}{k^2} \,\mathrm{d}k = \hat{\boldsymbol{e}} \cdot \boldsymbol{\gamma}_{\mathrm{e}} \cdot \hat{\boldsymbol{e}}, \tag{4.1}$$

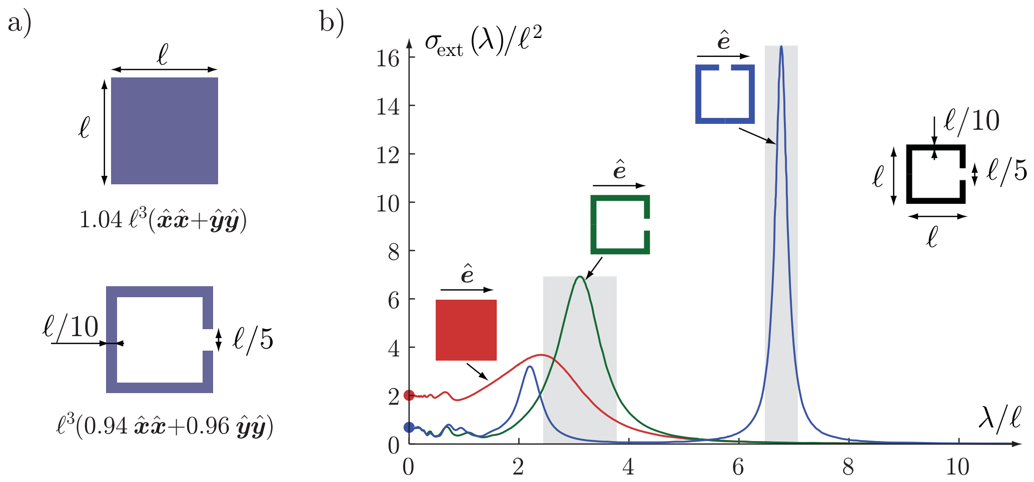

Figure 4: Illustrations of the polarizability dyadics (a) and extinction cross section (b) for perfectly conducting square patches and split rings with $\hat{\boldsymbol{k}} = \hat{\boldsymbol{z}}$.

where, if necessary, the integral in the center is a generalized integral defined as the limit of the integral to the left. It is often convenient to use the wavelength $\lambda = 2\pi/k$ to express the identity as the integrated extinction [26]

$$\frac{1}{\pi^2}\int_0^\infty \sigma_{\mathrm{ext}}(\lambda;\hat{\boldsymbol{k}},\hat{\boldsymbol{e}})\,\mathrm{d}\lambda = \hat{\boldsymbol{e}}\cdot\boldsymbol{\gamma}_{\mathrm{e}}\cdot\hat{\boldsymbol{e}}, \tag{4.2}$$

where the symbol σ_{ext} is reused to denote the extinction cross section as a function of the wavelength. This shows that the extinctions cross section integrated over all wavelengths is proportional to the polarizability $\hat{\boldsymbol{e}}\cdot\boldsymbol{\gamma}_{\mathrm{e}}\cdot\hat{\boldsymbol{e}}$.

It is known that $\boldsymbol{\gamma}_{\mathrm{e}}$ is monotone in the material parameters [14, 24]. That is $\boldsymbol{\gamma}_{\mathrm{e1}} \leq \boldsymbol{\gamma}_{\mathrm{e2}}$ if $\boldsymbol{\epsilon}_1(\boldsymbol{r}) \leq \boldsymbol{\epsilon}_2(\boldsymbol{r})$ for all points $\boldsymbol{r}$ in the object, where the inequality means $\boldsymbol{\gamma}_{\mathrm{e1}} \leq \boldsymbol{\gamma}_{\mathrm{e2}}$ if $\hat{\boldsymbol{e}}\cdot(\boldsymbol{\gamma}_{\mathrm{e2}}-\boldsymbol{\gamma}_{\mathrm{e1}})\cdot\hat{\boldsymbol{e}} \geq 0$ for all $\hat{\boldsymbol{e}} \in \mathbb{R}^3$. It is hence convenient to introduce the high contrast polarizability dyadic $\boldsymbol{\gamma}_\infty$ such that $\boldsymbol{\gamma}_{\mathrm{e}} \leq \boldsymbol{\gamma}_\infty$ for all objects confined to the same volume [26]. The high contrast polarizability dyadics are illustrated for a square patch and a square split ring resonator in Fig. 4a. Note that $\boldsymbol{\gamma}_\infty$ is larger for the patch than for the split ring as the patch can be constructed from the split ring by adding material. The variational principle together with the sum rule (4.2) show that the integrated extinction is monotone in the material parameters.

Bound the integral (4.2) as

$$|\Lambda| \min_{\lambda\in\Lambda} \sigma_{\mathrm{ext}}(\lambda;\hat{\boldsymbol{k}},\hat{\boldsymbol{e}}) \leq \pi^2 \hat{\boldsymbol{e}}\cdot\boldsymbol{\gamma}_{\mathrm{e}}\cdot\hat{\boldsymbol{e}}, \tag{4.3}$$

where $\Lambda = [\lambda_1, \lambda_2]$ and $|\Lambda| = \lambda_2 - \lambda_1$ to get a simple bound on the bandwidth times the extinction cross section [26]. The bounds are illustrated by the shaded boxes in Fig. 4, that are constructed to have similar total areas as the areas under the corresponding curves. An interpretation of the bound is that it is not possible to design a scatterer with $\sigma_{\mathrm{ext}}(\lambda)$ that does not intersect the box.

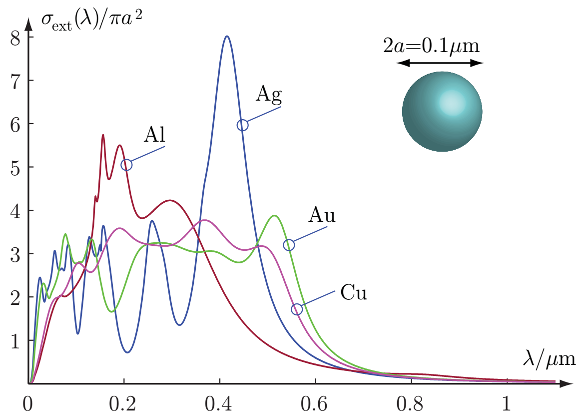

Figure 5: Extinction cross sections for aluminum (Al), silver (Ag), gold (Au), and copper (Cu) spheres with radius $a = 50\,\text{nm}$.

A second example is provided by spherical scatterers composed of aluminum (Al), silver (Ag), gold (Au), and copper (Cu), using the permittivity models in [29]. The extinction cross sections for spheres with radius $a = 50\,\text{nm}$ are depicted in Fig. 5 as functions of the wavelength λ. It is observed that σ_{ext} is large compared to the cross section area πa^2 at some resonance wavelengths and that σ_{ext} is small for $\lambda > 1\,\mu\text{m}$ and $\sigma_{\text{ext}}(\lambda) \to 0$ as $\lambda \to 0$. The polarizabilities of the spheres are $\boldsymbol{\gamma}_{\text{e}} = \boldsymbol{\gamma}_\infty = 4\pi a^3\mathbf{I}$ as they have a static conductivity. This is also confirmed by numerical integration of the sum rule (4.2). The areas under the curves defined by $\sigma_{\text{ext}}(\lambda)$ are hence given by the radii of the spheres. The dispersion characteristics of the materials distribute the area to different wavelengths. The large values of $\sigma_{\text{ext}}(\lambda)$ for silver around $\lambda \approx 0.4\,\mu\text{m}$ must hence be compensated by reduced values at other wavelengths as seen in the figure. A comparison with the bound (4.3) shows that

$$\lambda_2 \frac{\min_{\lambda\in\Lambda} \sigma_{\text{ext}}(\lambda; \hat{\boldsymbol{k}}, \hat{\boldsymbol{e}})}{\pi a^2} \leq 4\pi^2 a \approx 2\,\mu\text{m} \tag{4.4}$$

if $\lambda_1 = 0$ is used. This gives a rough estimate of the average distribution of σ_{ext}, *e.g.*, $\sigma_{\text{ext}}/\pi a^2 = 3$ gives $\lambda_2 = 2/3\,\mu\text{m}$.

The polarizabilities of hollow and solid metallic spheres are identical due to the static conductivity of metals [17]. This imply that the integrated extinctions (4.2) are identical for hollow and solid spheres composed of metallic materials. The extinction cross sections of hollow silver spheres with outer radius $a = 50\,\text{nm}$ and inner radii $0.5a$ and $0.9a$ are depicted in Fig. 6. Note that the increased values of $\sigma_{\text{ext}}(\lambda)$ around $0.7\,\mu\text{m}$ are compensated by low values at the shorter wavelengths.

5 Conclusions

A time-domain approach is used to derive the forward-scattering sum rule. The time-domain analysis highlights the used assumptions such as causality and passivity. The use of causality is clearly observed in the definition of the forward-scattering

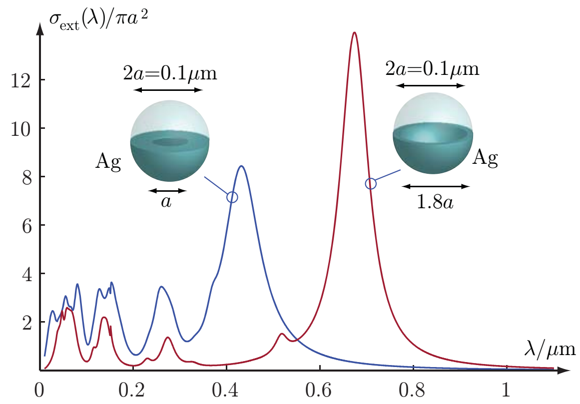

Figure 6: Extinction cross sections for layered silver spheres with outer radius $a = 50\,\mathrm{nm}$ and inner radii $0.5a$ and $0.9a$.

impulse response. It follows from the fact that the wave-front speed cannot exceed the speed of light in free space. Passivity enters though conservation of energy that states that the extincted energy is non-negative. This also shows that the impulse response is the kernel of a passive convolution operator, and, hence, constructs a Herglotz function in the Fourier domain [31].

The forward scattering sum rule has previously been used to derive bounds on scattering and absorption of metamaterials [27, 28], antenna bandwidth and directivity [9, 10], and extraordinary transmission of power though sub-wavelength apertures [12]. Here, the sum rule and bounds are exemplified for resonant perfectly conducting structures and spheres composed of various metals. It is observed that the sum rule offers simple estimates of the overall behavior of the extinction-cross section, $\sigma_{\mathrm{ext}}(\lambda)$, in a way that the dispersion characteristics of the metals determine the resonances but the (long-wavelength) polarizability dyadic determines the total area under the curve $\sigma_{\mathrm{ext}}(\lambda)$. This is particularly important in *e.g.*, cloaking of objects in free space [1], where it is noted that the cloaking material increases the polarizability as it adds material [14, 24] and hence the area under $\sigma_{\mathrm{ext}}(\lambda)$. Reduction of $\sigma_{\mathrm{ext}}(\lambda)$ at some desired wavelengths must then be compensated by increased values of $\sigma_{\mathrm{ext}}(\lambda)$ at other wavelengths.

Integral representation of the scattered field Here, some classical integral representations are summarized, see *e.g.*, [30]. The electric field is

$$\widetilde{\boldsymbol{E}}_{\mathrm{s}}(k,\boldsymbol{r}) = \mathrm{e}^{\mathrm{i}kr}\frac{\widetilde{\boldsymbol{F}}(k,\hat{\boldsymbol{r}})}{r} + \mathcal{O}(r^{-2}) \quad \text{as } r\to\infty \tag{.1}$$

in the far-field region. The volume integral representation of the far field from a current distribution is

$$\widetilde{\boldsymbol{F}}(k,\hat{\boldsymbol{r}}) = \frac{\mathrm{i}k\eta_0}{4\pi}\hat{\boldsymbol{r}}\times\left(\int_V \mathrm{e}^{-\mathrm{i}k\hat{\boldsymbol{r}}\cdot\boldsymbol{r}}\widetilde{\boldsymbol{J}}(k,\boldsymbol{r})\,\mathrm{dV}\times\hat{\boldsymbol{r}}\right) \tag{.2}$$

that is used in the derivation of the low-frequency asymptotic expansions (3.5).

The surface integral representation is used in the definition of the impulse response, h_{t} in (2.4) and the transfer function $h(k) = 4\pi\hat{\boldsymbol{e}}\cdot\widetilde{\boldsymbol{F}}^{(\delta)}(k,\hat{\boldsymbol{k}})/k$, in (3.4). It is given by

$$\widetilde{\boldsymbol{F}}^{(\delta)}(k,\hat{\boldsymbol{k}}) = \frac{\mathrm{i}k}{4\pi}\hat{\boldsymbol{k}}\times\int_{\partial V}\big(\hat{\boldsymbol{n}}(\boldsymbol{r})\times\widetilde{\boldsymbol{E}}_{\mathrm{s}}^{(\delta)}(k,\boldsymbol{r})-\eta_0\hat{\boldsymbol{k}}\times(\hat{\boldsymbol{n}}(\boldsymbol{r})\times\widetilde{\boldsymbol{H}}_{\mathrm{s}}^{(\delta)}(k,\boldsymbol{r}))\big)\mathrm{e}^{-\mathrm{i}k\hat{\boldsymbol{k}}\cdot\boldsymbol{r}}\,\mathrm{dS} \quad (.3)$$

that gives the function ($\hat{\boldsymbol{e}}\cdot\hat{\boldsymbol{k}}=0$)

$$\begin{aligned} h(k) &= \mathrm{i}\hat{\boldsymbol{e}}\cdot\hat{\boldsymbol{k}}\times\int_{\partial V}\big(\hat{\boldsymbol{n}}(\boldsymbol{r})\times\widetilde{\boldsymbol{E}}_{\mathrm{s}}^{(\delta)}(k,\boldsymbol{r})-\eta_0\hat{\boldsymbol{k}}\times(\hat{\boldsymbol{n}}(\boldsymbol{r})\times\widetilde{\boldsymbol{H}}_{\mathrm{s}}^{(\delta)}(k,\boldsymbol{r}))\big)\mathrm{e}^{-\mathrm{i}k\hat{\boldsymbol{k}}\cdot\boldsymbol{r}}\,\mathrm{dS} \\ &= \mathrm{i}\hat{\boldsymbol{e}}\cdot\int_{\partial V}\big(\hat{\boldsymbol{k}}\times(\hat{\boldsymbol{n}}(\boldsymbol{r})\times\widetilde{\boldsymbol{E}}_{\mathrm{s}}^{(\delta)}(k,\boldsymbol{r}))+\eta_0\hat{\boldsymbol{n}}(\boldsymbol{r})\times\widetilde{\boldsymbol{H}}_{\mathrm{s}}^{(\delta)}(k,\boldsymbol{r})\big)\mathrm{e}^{-\mathrm{i}k\hat{\boldsymbol{k}}\cdot\boldsymbol{r}}\,\mathrm{dS} \quad (.4)\end{aligned}$$

in the Fourier domain. The corresponding time-domain case is obtained by an inverse Fourier transform, *i.e.*,

$$\boldsymbol{E}_{\mathrm{s}}(t,\boldsymbol{r}) = \frac{\mathrm{c}_0}{2\pi}\int_{\mathbb{R}}\widetilde{\boldsymbol{E}}_{\mathrm{s}}(k,\boldsymbol{r})\mathrm{e}^{-\mathrm{i}kt\mathrm{c}_0}\,\mathrm{d}k \quad (.5)$$

that gives

$$\begin{aligned}\boldsymbol{F}^{(\delta)}(t,\hat{\boldsymbol{k}}) = -\frac{\partial}{\partial t}\frac{\hat{\boldsymbol{k}}\times}{4\pi\mathrm{c}_0}\int_{\partial V}&\hat{\boldsymbol{n}}(\boldsymbol{r})\times\boldsymbol{E}_{\mathrm{s}}^{(\delta)}(t+\frac{\boldsymbol{r}\cdot\hat{\boldsymbol{k}}}{\mathrm{c}_0},\boldsymbol{r}) \\ &-\eta_0\hat{\boldsymbol{k}}\times(\hat{\boldsymbol{n}}(\boldsymbol{r})\times\boldsymbol{H}_{\mathrm{s}}^{(\delta)}(t+\frac{\boldsymbol{r}\cdot\hat{\boldsymbol{k}}}{\mathrm{c}_0},\boldsymbol{r}))\,\mathrm{dS}\,. \quad (.6)\end{aligned}$$

The time-domain co-polarized case in the forward direction is

$$\hat{\boldsymbol{e}}\cdot\boldsymbol{F}^{(\delta)}(t,\hat{\boldsymbol{k}}) = -\frac{1}{4\pi\mathrm{c}_0}\frac{\partial h_{\mathrm{t}}}{\partial t}, \quad (.7)$$

where

$$h_{\mathrm{t}}(t) = \hat{\boldsymbol{e}}\cdot\int_{\partial V}\hat{\boldsymbol{k}}\times\big(\hat{\boldsymbol{n}}(\boldsymbol{r})\times\boldsymbol{E}_{\mathrm{s}}^{(\delta)}(t+\frac{\boldsymbol{r}\cdot\hat{\boldsymbol{k}}}{\mathrm{c}_0},\boldsymbol{r})\big)+\eta_0\hat{\boldsymbol{n}}(\boldsymbol{r})\times\boldsymbol{H}_{\mathrm{s}}^{(\delta)}(t+\frac{\boldsymbol{r}\cdot\hat{\boldsymbol{k}}}{\mathrm{c}_0},\boldsymbol{r})\,\mathrm{dS}\,. \quad (.8)$$

References

[1] A. Alù and N. Engheta. Theory and potentials of multi-layered plasmonic covers for multi-frequency cloaking. *New Journal of Physics*, **10**, 115036, 2008.

[2] A. Bernland, A. Luger, and M. Gustafsson. Sum rules and constraints on passive systems. Technical Report LUTEDX/(TEAT-7193)/1-28/(2010), Lund University, Department of Electrical and Information Technology, P.O. Box 118, S-221 00 Lund, Sweden, 2010. `http://www.eit.lth.se`.

[3] A. T. de Hoop. A time domain energy theorem for scattering of plane electromagnetic waves. *Radio Sci.*, **19**, 1179–1184, 1984.

[4] A. Derneryd, M. Gustafsson, G. Kristensson, and C. Sohl. Application of gain-bandwidth bounds on loaded dipoles. *IET Microwaves, Antennas & Propagation*, **3**(6), 959–966, 2009.

[5] W. F. Donoghue, Jr. *Distributions and Fourier Transforms.* Academic Press, New York, 1969.

[6] L. C. Evans. *Partial Differential Equations.* American Mathematical Society, Providence, Rhode Island, 1998.

[7] R. M. Fano. Theoretical limitations on the broadband matching of arbitrary impedances. *Journal of the Franklin Institute*, **249**(1,2), 57–83 and 139–154, 1950.

[8] E. A. Guillemin. *The Mathematics of Circuit Analysis.* MIT Press, 1949.

[9] M. Gustafsson, C. Sohl, and G. Kristensson. Physical limitations on antennas of arbitrary shape. *Proc. R. Soc. A*, **463**, 2589–2607, 2007.

[10] M. Gustafsson, C. Sohl, and G. Kristensson. Illustrations of new physical bounds on linearly polarized antennas. *IEEE Trans. Antennas Propagat.*, **57**(5), 1319–1327, May 2009.

[11] M. Gustafsson. On the non-uniqueness of the electromagnetic instantaneous response. *J. Phys. A: Math. Gen.*, **36**, 1743–1758, 2003.

[12] M. Gustafsson. Sum rule for the transmission cross section of apertures in thin opaque screens. *Opt. Lett.*, **34**(13), 2003–2005, 2009.

[13] J. D. Jackson. *Classical Electrodynamics.* John Wiley & Sons, New York, second edition, 1975.

[14] D. S. Jones. Scattering by inhomogeneous dielectric particles. *Quart. J. Mech. Appl. Math.*, **38**, 135–155, 1985.

[15] A. Karlsson. On the time domain version of the optical theorem. *Am. J. Phys*, **68**(4), 344–349, 2000.

[16] F. W. King. *Hilbert Transforms, Volume 2.* Cambridge University Press, 2009.

[17] R. E. Kleinman and T. B. A. Senior. Rayleigh scattering. In V. V. Varadan and V. K. Varadan, editors, *Low and high frequency asymptotics*, volume 2 of *Handbook on Acoustic, Electromagnetic and Elastic Wave Scattering*, chapter 1, pages 1–70. Elsevier Science Publishers, Amsterdam, 1986.

[18] H.-O. Kreiss and J. Lorenz. *Initial-Boundary Value Problems and the Navier-Stokes Equations.* Academic Press, San Diego, 1989.

[19] R. G. Newton. *Scattering Theory of Waves and Particles.* Dover Publications, New York, second edition, 2002.

[20] H. M. Nussenzveig. *Causality and dispersion relations.* Academic Press, London, 1972.

[21] W. K. Panofsky and M. Phillips. *Classical Electricity and Magnetism.* Addison-Wesley, Reading, MA, USA, second edition, 1962.

[22] E. M. Purcell. On the absorption and emission of light by interstellar grains. *J. Astrophys.*, **158**, 433–440, 1969.

[23] M. Reed and B. Simon. *Methods of modern mathematical physics*, volume II: Fourier analysis, Self-adjointness. Academic Press, New York, 1975.

[24] D. Sjöberg. Variational principles for the static electric and magnetic polarizabilities of anisotropic media with perfect electric conductor inclusions. *J. Phys. A: Math. Theor.*, **42**, 335403, 2009.

[25] C. Sohl and M. Gustafsson. A priori estimates on the partial realized gain of Ultra-Wideband (UWB) antennas. *Quart. J. Mech. Appl. Math.*, **61**(3), 415–430, 2008.

[26] C. Sohl, M. Gustafsson, and G. Kristensson. Physical limitations on broadband scattering by heterogeneous obstacles. *J. Phys. A: Math. Theor.*, **40**, 11165–11182, 2007.

[27] C. Sohl, M. Gustafsson, and G. Kristensson. Physical limitations on metamaterials: Restrictions on scattering and absorption over a frequency interval. *J. Phys. D: Applied Phys.*, **40**, 7146–7151, 2007.

[28] C. Sohl, C. Larsson, M. Gustafsson, and G. Kristensson. A scattering and absorption identity for metamaterials: experimental results and comparison with theory. *J. Appl. Phys.*, **103**(5), 054906, 2008.

[29] B. Ung and Y. Sheng. Interference of surface waves in a metallic nanoslit. *Optics Express*, **15**(3), 1182–1190, 2007.

[30] J. van Bladel. *Electromagnetic Fields.* IEEE Press, Piscataway, NJ, second edition, 2007.

[31] A. H. Zemanian. *Realizability Theory for Continuous Linear Systems.* Dover Publications, New York, 1995.